VARIATIONS IN IONOSPHERIC D-REGION RECOMBINATION PROPERTIES DURING INCREASE OF ITS X-RAY HEATING INDUCED BY SOLAR X-RAY FLARE

by

Aleksandra M. NINA[a*], Vladimir M. ČADEŽ[b], Maša D. LAKIĆEVIĆ[b], Milan M. RADOVANOVIĆ[c,d], Aleksandra B. KOLARSKI[e], and Luka Č. POPOVIĆ[b,f]

[a] Institute of Physics Belgrade, University of Belgrade, Belgrade, Serbia
[b] Astronomical Observatory of Belgrade, Belgrade, Serbia
[c] Geographical Institute Jovan Cvijić SASA, Belgrade, Serbia
[d] South Ural State University, Institute of Sports, Tourism and Service, Chelyabinsk, Russia
[e] STC NIS-Naftagas LLC, Novi Sad, Serbia
[f] Faculty of Science, University of Banja Luka, Banja Luka, Republic of Srpska, Bosnia and Herzegovina

Original scientific paper
https://doi.org/10.2298/TSCI190501313N

In this paper we present an analysis of parameters describing the effective recombination processes in the upper ionospheric D-region in the period of its additional heating by the X-radiation emitted during a solar X-ray flare. We present a procedure for calculation of the effective recombination coefficient and electron loss rate in the period when the X-radiation flux detected by the GOES satellite in the wavelength domain between 0.1 and 0.8 nm increases. The developed procedure is based on observational data obtained in the low ionospheric monitoring by the very low/low frequency radio waves and it is related to the considered area and time period. The obtained expressions are applied to data for the very low frequency signal emitted in Germany and recorded in Serbia during the solar X-ray flare detected by the GOES-14 satellite on May 5, 2010.

Key words: *effective recombination coefficient, electron loss rate, ionospheric D-region, solar X-ray flares*

Introduction

Due to influences of numerous geo and astrophysical phenomena, the thermal properties of the ionosphere can significantly vary in time. One of the most important phenomena which induce intensive low ionospheric disturbances is emission of high-energy electromagnetic radiation from the Sun in the X-spectral domain called a solar X-ray flare. This radiation primarily disturbs the ionospheric plasma in the D-region (60-90 km) and research of these effects is a subject of many studies [1-4]. Earlier investigations show that changes in plasma parameters induced by these astrophysical phenomena depend on the radiation intensity as well as on the atmospheric properties (see for example [5]) and that relative changes of plasma parameters due to heating by high-energy photons can reach a few orders of magnitude.

* Corresponding author, e-mail: sandrast@ipb.ac.rs

Because of complexity of radiation characteristics and processes in Earth's atmosphere, analysis of space and time distributions of a particular parameter require different approximations. Consequently, divisions in both space and time domains are necessary for many studies. In the case of the ionospheric D-region, which is in the focus of this research, the differences in modeling depending on the altitude are mainly consequences of variation of dominant electron loss processes. Namely, in the upper part, the recombination processes can be considered as the most important in reduction of the electron density while electron attachment processes have dominant role in the lowest D-region altitudes [6]. On the other side, approximations which can be applied to different parameters depend on the flare phase. For this reason, many studies are related to quiet conditions or the relaxation period [7, 8], time of radiation flux maximum [6, 9], *etc.*

Although solar X-ray flares can provide significant variations in the D-region properties which are connected with thermal processes, research of temperature dependent parameters during disturbed conditions are not enough analyzed. In this paper we investigate the influence of the X-radiation increase on parameters describing recombination processes in the D-region part between 75 km and 80 km. First, we give a new procedure for calculation of time evolution of the effective recombination coefficient which describes the dominant processes in the electron density reduction within the considered altitude domain. This procedure is based on experimental very low frequency/low frequency (VLF/LF) data and long-wave propagation capability (LWPC) numerical model for simulation of the VLF/LF signal propagation [10] and it follows the research presented in [5] and [7] and references therein. In the second part we analyze properties of the electron loss rate in the considered altitude domain. We consider the time period when the X-radiation intensity increases to its maximum value. The obtained theoretical equations are applied to a particular case of the D-region perturbation induced by the solar X-ray flare of class C8.8 occurred on May 5, 2010. It is interesting that this flare was in the beginning of NASA Solar Dynamics Observatory (SDO) observations and that its characteristics are very well analyzed [11].

Experimental set-up, observations and data processing

The presented study requires data obtained in observations of the solar X-ray radiation and in the D-region monitoring which can be obtained by a GOES satellite and ionospheric sounding by the VLF/LF radio signals, respectively.

For general descriptions of the space-time dependencies of plasma parameters located in the considered area, it is practically sufficient to consider one particular flare event. Namely, the major characteristics of the D-region response to the solar X-ray flares are very similar (see for example comparison given in [7]) and statistical analyses give additional information related only to dependencies of the considered values on the ionospheric state and radiation properties. In this study the major goal is determination of expressions for time evolution of plasma parameters (the effective recombination coefficient α_{eff} and electron loss rate L) which allow us to use one particular flare event as an example. Here we chose to study the perturbation induced by the solar X-flare occurred on May 5, 2010 with photon flux I registered by the GOES-14 satellite of National Oceanic and Atmospheric Administration (NOAA), USA (fig. 1, upper panel) at the wavelengths range 0.1-0.8 nm for two reasons: this is the best example of the dominant influence of a solar X-ray on the D-region (seen in fig. 1 as very flat amplitude and phase time evolutions, as recorded by the AWESOME VLF receiver [12], which correspond to time evolution of the X-radiation time evolution and this study is an extension of complementary research given in [7, 8] related to the unperturbed conditions and relaxation period, respectively. Due

to the first reason this flare has also been considered in several previous investigations (see [13] and references therein). One of the open questions of this study is related to research of the radiation and atmospheric properties on the electron reduction in the considered flare phase. This task exceeds the topic of this paper and should be a subject of the incoming research.

The time evolution of the solar X-ray radiation is important for determination of the time period within the ionospheric parameters that should be analyzed. In fig. 1 it is seen that the flux increase is recorded from about 10:48 UT to near 11:53 UT. However, the beginning of the considered period is chosen to be about 11:49 UT because of the time delay of the ionospheric response (seen as the beginning of variations in signal amplitude A_{rec} and phase P_{rec}) with respect to the start of the flare occurrence.

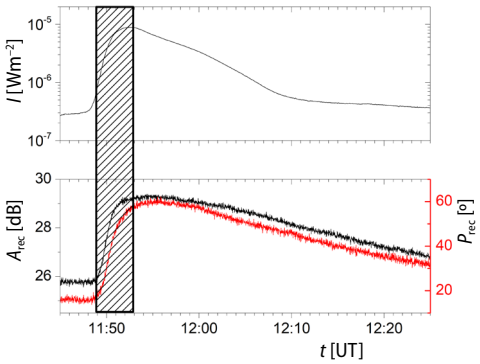

Figure 1. Increase of the X-radiation flux recorded by the GOES-14 satellite at wavelengths domain 0.1-0.8 nm (upper panel) and reaction of the phase and amplitude (bottom panel) of the VLF signal emitted by the DHO transmitter located in Germany and received by the AWESOME receiver in Serbia. The shaded domain represents the considered period analyzed when the recorded X-radiation flux increases in time after beginning of the ionospheric response

Processing of the recorded amplitude and phase (using the LWPC numerical model for simulation of the VLF signal propagation [10]) is directed to determination of Wait's parameters *sharpness* β [km^{-1}] and signal reflection height H' [km] which are required for calculation of the electron density $N_e(h,t)$ [m^{-3}] at fixed altitude h [km] using Wait's model [14] and expression given in [15]:

$$N_e(h,t) = 1.43 \cdot 10^{13} \, \mathrm{e}^{-\beta(t)H'(t)} \mathrm{e}^{[\beta(t)-0.15]h} \tag{1}$$

which is the standard procedure applied in numerous studies of the low ionospheric disturbances induced by different events [6, 16, 17].

The Wait's parameters are modeled using criteria given in [16] and applied in many papers [6, 18, 19]. The obtained values and the relevant fitted curves (polynomial functions of the order 4) are shown in fig. 2 (upper panel). The surface plot of the electron density time and altitude dependences, shown in the bottom panel of this figure, are in agreement with relevant data presented in [6, 9, 16].

D-region modelling

In the upper horizontal uniform D-region, where the recombination processes dominate in the free electron number reduction, the electron density dynamics can be described by expression [20]:

$$\frac{\mathrm{d}N_e(h,t)}{\mathrm{d}t} = G_0(h) + K(h,t)I(t) - \alpha_{\mathrm{eff}}(h,t)N_e^2(h,t) \tag{2}$$

where $G_0(h)$ is the electron gain rate in the unperturbed D-region at altitude, h, whose determination is explained in details in [7], $I(t)$ – the X-radiation flux detected by the GOES satellite in energy channel for wavelengths between 0.1 nm and 0.8 nm at time, t. The coefficient $K(h, t)$ is a space and time dependent scaling coefficient described in [5] while α_{eff} is the effective re-

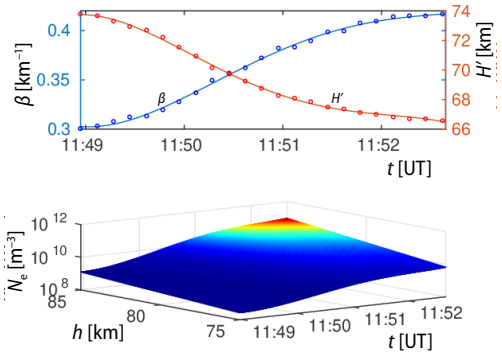

Figure 2. Time evolutions of Wait's parameters (upper panel) and the electron density in the altitude domain between 75 km and 85 km (bottom panel) for the considered X-ray flare event

combination coefficient that also vary in space and time.

Although we can neglect transport processes (they become important at altitudes above 120-150 km [21]) and although the time and altitude dependencies of $N_e(h,t)$ and $G_0(h)$ in the horizontal uniform ionosphere can be determined, eq. (2) is very complex because of lack of observational data needed for calculation of the coefficients K and α_{eff} during the disturbance. For this reason, it is necessary to use some approximations for one of these parameters.

In this study we use the previous research presented in [7] and [22] to model the effective recombination coefficient time evolutions at the upper D-region heights. The developed procedure and the obtained results open possibility for further modeling other plasma parameters in the upper part of the D-region disturbed by the solar X-ray flare and they enable study of the flare phase between its maximum flux and recombination regime which will be in focus of our upcoming research.

Modelling the time evolution of the effective recombination coefficient

As we already said, determination of the time evolution of the effective recombination coefficient is a very complex task and, due to lack of real observations which are necessary for calculation of plasma parameters at the considered location and time period, it is necessary to use some approximations. In this study we present a model for calculation of the effective recombination coefficient at altitude domain between 75 km and 85 km during increase of the X-ray flux. Our procedure is divided in three steps:

– Determination of an analytical expression for dependency of the effective recombination coefficient on the X-ray flux at a fixed altitude using data given in literature,
– Correction of the obtained dependence on calculated effective recombination coefficient in quiet conditions obtained from a real low ionospheric observation relevant to the considered case and transformation of the flux dependency in time evolution of the effective recombination coefficient corrected to the initial condition for the considered case.
– Correction of the obtained dependency on the calculated effective recombination coefficient in the maximum X-radiation flux obtained from a real low ionospheric observation relevant to the considered case.

In this way, we provide a model for calculation of the effective recombination coefficient based on real observations which means that the obtained values are related to the considered event and the observed area.

Dependence of effective recombination coefficient on X-ray flux

Research presented in [5] shows that dependence of the electron density and its time derivative on the X-ray flux detected by the GOES satellite has complex shapes. However, in the period between times of relatively small increase of the electron density and maximum of the considered X-radiation flux these dependences are very close to linear dependences in the exp-exp scale. Furthermore, the time evolution of radiation at wavelengths which dominate

in ionization in the upper ionosphere indicates that the expected variations in the parameter K near the radiation maximum (primarily induced by variation in the X-radiation spectrum) is not significant. Because of these properties and assuming that ionization without the X-radiation, $G_0(h)$, is stationary (*e. g.* that X-radiation is the dominant source of the ionization rate increase) we assumed that the fitted dependence of the effective recombination coefficient in maxima of the X-radiation fluxes detected by the GOES satellite at the wavelength domain 0.1-0.8 nm for different flare events can be used as the dependence of this plasma parameter on the X-radiation flux during its increase in one particular X-ray flare event. Here we consider the X-ray flux detected by the GOES energy channel for the wavelength domain 0.1-0.8 nm because it better describes the X-ray photoionization in the upper D-region than the other energy channel (0.05-0.4 nm) [5].

Dependencies of the effective recombination coefficient in the X-radiation flux maxima is given in several studies [6, 22, 23]. In our investigation we use the results presented in [22] which are related to the altitude of 80 km. As seen in fig. 3, the influence of the radiation characteristics and atmospheric conditions relevant for different flare events is important. For this reason, we fit these values to estimate the analytical expression for the $\psi_{\text{eff}}(\Phi)$ dependence at this altitude. Here we notice that the letters ψ and Φ are used for the effective recombination coefficient and X-radiation flux in the maximum X-radiation of events analyzed in [22] to indicate the difference of these parameters from those calculated by data obtained in real observations of the particular studied events which are designated as α and I, respectively. To choose the fitting function for fit data given in [22] we use the criterion that $\psi_{\text{eff}}(\Phi)$ should saturate going to lower fluxes *e. g.* going to quiet conditions. In fig. 3 we show the obtained fitted curves for $\log(\psi^*)(\log(\Phi^*))$ by formula:

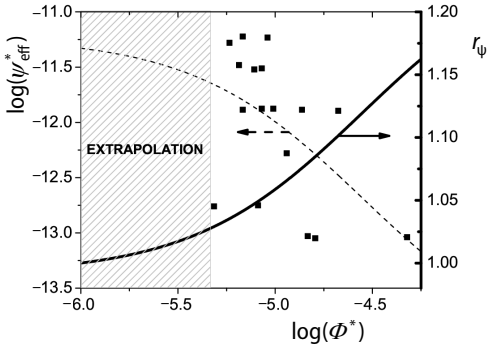

Figure 3. Left axis: Dependences of ψ_{eff} normalized to its unit values 1 m^3s^{-1} on the X-radiation flux normalized to its unit values 1 Wm^{-2}. Scatters represent values obtained in [22] while dashed line is obtained by fitting these values with eq. (3). Right axis: tick solid line represents normalized values of fitted curve on value of $\log(\psi^*_{\text{eff}})$ related to quiet state. These calculations are made using eq. (4)

$$\log(\psi^*_{\text{eff}}) = -14.13109 + \frac{-11.2868 + 14.13109}{1 + 10^{\log(\phi^*) - \log(-11.32906)}} \tag{3}$$

Here we fitted the logarithmic values of the considered physical parameters divided by relevant unique values, $\log(\psi^*_{\text{eff}}) = \log(\psi_{\text{eff}}\ /1\ m^3s^{-1})$ and $\log(\Phi^*) = \log(\Phi^*/1\ Wm^{-2})$, to obtain better determination of representative fits related to values which lies within more than one order of magnitude.

The fact that the considered altitude domain is characterized by very similar processes allows us to use eq. (3) as approximation in the entire considered altitude domain. This assumption is in agreement with results obtained in [23].

The obtained values are relevant for the set of data given in [22] that describes specific conditions in the ionosphere relevant for the events analyzed in that study. To obtain the procedure for determination the dependence of the effective recombination coefficient on the radiation flux (or in other words, to reduce the influence of the considered geographical locations and

other parameters), in our model we modified the fitted curve using observational data relevant to quiet conditions and values at the moment of the radiation flux maximum for the considered X-ray flare and observed D-region area.

Correction on the quiet condition

To fit the obtained curve to the values obtained by real observations we first normalize the dependence $\log(\psi^{o}_{\text{eff}})$ given by eq. (3) on its value relevant for the unperturbed conditions $\log(\psi^{o}_{\text{eff}})$:

$$r_{\psi^*} = \frac{\log[\psi^{*}_{\text{eff}}(\Phi)]}{\log(\psi^{o*}_{\text{eff}})} \tag{4}$$

This expression gives us the final information from the data given in [22] and it is further used as an input set of data for calculation the time evolution of this plasma parameter for the considered flare event.

The next step in our procedure is applying eq. (4) (dependent on flux) in calculation of the first correction coefficient, r^{o}, (describing the correction on the initial unperturbed conditions) which is time dependent. To do that, we use the GOES satellite data set for the X-ray flux time evolution and find pairs of parameters t and Φ specific for the considered flare event. These parameters allow us to transform the energy dependence that is given in eq. (4) and shown in fig. 3 to r^{o}: $r_{\psi^*}(\Phi) \rightarrow r^{o}(t)$. Here we notice that transformation should first be made for the relevant form with logarithm expressions and after that, using the exponential function, the required corrected parameter should be calculated.

The product of coefficient, r^{o}, and the initial effective recombination coefficient α^{o}_{eff} gives the effective recombination coefficient corrected only to the unperturbed conditions. Here, α^{o}_{eff} can be determined from eq. (2) assuming $\mathrm{d}N_e/\mathrm{d}t \approx 0$ and $G_0(h) >> K(h, t)I(t)$.

$$\alpha^{o}_{\text{eff}}(h) = \frac{G_0(h)}{N^{o2}_{e}(h)} \tag{5}$$

where N^{o}_{e} represents the electron density in the quiet ionospheric D-region. As we already said, N^{o}_{e} and $G_0(h)$ can be obtained by procedures explained in [7] and [15], respectively.

Correction on properties at time of the X-radiation flux maximum

In the second correction we normalize the obtained dependence by function r:

$$r = \frac{\Phi - \Phi^{o}}{\Phi^{(\text{Imax})} - \Phi^{o}} r^{(\text{Imax})} \tag{6}$$

which fits the modeled effective recombination coefficient corrected on quiet conditions in procedure explained in section *Correction on the quiet condition* to its value α_{eff} obtained in the modeling based on real observation of the analyzed event at the time of the X-radiation intensity maximum. Here, $\Phi^{(\text{Imax})}$ and $r^{(\text{Imax})}$ are Φ and r at the time of the X-radiation intensity maximum, respectively.

Similarly like in the procedure given for the first correction, $\alpha^{\text{Imax}}_{\text{eff}}$ can be obtained from eq. (2). As we here consider the maximum of the X-radiation, we can assume that the time derivative of KI is equal to 0. In addition, from the fact that the electron reduction rate still increases in this period [24] we can conclude that N_e^2 (it increases in time) dominates α_{eff} in time

variation of this term *e. g.* that $d\alpha_{eff}/dt < dN_e^2/dt$. For this reason, we use $d(\alpha_{eff}N_e^2)/dt \approx \alpha_{eff}dN_e^2/dt$. By these assumptions, the time derivative of eq. (2) gives:

$$\alpha_{\text{eff}}^{\text{Imax}}(h) = -\frac{\mathrm{d}^2 N_e(h,t)}{\mathrm{d}t^2}\left[\frac{\mathrm{d}N_e^2(h,t)}{\mathrm{d}t}\right]^{-1}\Bigg|_{t=t_{\text{Imax}}} \tag{7}$$

Finally, the obtained expression for the effective recombination coefficient is:

$$\alpha_{\text{eff}}^{\text{Imax}}(h) = C(h)\alpha_{\text{eff}}^{o}(h) \tag{8}$$

where normalized coefficient C is given by:

$$C = \frac{\Phi - \Phi^o}{\Phi^{(\text{Imax})} - \Phi^o} r^o r^{(\text{Imax})} \tag{9}$$

Modeling of the electron loss rate

As one can see in eq. (2), knowledge of the electron density and effective recombination coefficient allows us to calculate the electron loss rate $L(h, t)$ using the expression:

$$L(h,t) = \alpha_{\text{eff}}(h,t)N_e^2(h,t) \tag{10}$$

where the electron recombination coefficient α_{eff} and the electron density N_e are given by eqs. (8) and (1), respectively.

Results and discussions

In this paper we apply the model presented in section *D-region modelling* to the X-ray flux data detected by the GOES-14 satellite and to data on the amplitude and phase of the 23.4 kHz signal emitted by the VLF transmitter in Germany and received by the Belgrade receiver station in Serbia. These values, recorded during the period of influence of the solar X-ray flare of class C8.8 occurred on May 5, 2010, are given in section *Experimental set-up, observations and data processing,* fig. 1.

As we can see in section *D-region modelling*, to determine the time evolution of the effective recombination coefficient it is necessary to know its values in quiet conditions and at the moment of the solar X-radiation maximum. Calculations based on eqs. (5) and (7) give the lower values of α_{eff} during a maximum of the radiation intensity than when the state is quasi stationary, and its variation within one order of magnitude at fixed altitude during the considered flare influence. In both cases α_{eff} decreases with altitude.

Although research of the altitude dependence of the coefficient α_{eff} is presented in several studies the comparison of obtained results is not simple due to variations with geographical position and periodical changes in quiet Sun radiation and unperturbed atmospheric properties. During perturbed periods, additional differences in atmospheric dynamic can be consequences of various X-radiation spectral characteristics. These deviations are visualized in [24, 25] where one can see that the presented values at fixed altitude can lie within about three orders of magnitude. However, it is important to point out that α_{eff} decreases with altitude, as visible in fig. 4, is also obtained in 8 of 10 and in 9 of 10 analyses shown in [24, 25], respectively.

The obtained values in the case of quiet conditions are in a good agreement with those presented in earlier investigations. In fig. 4 we can see that our model, applied to the considered conditions, gives a very similar shape in comparison with those shown in [26]

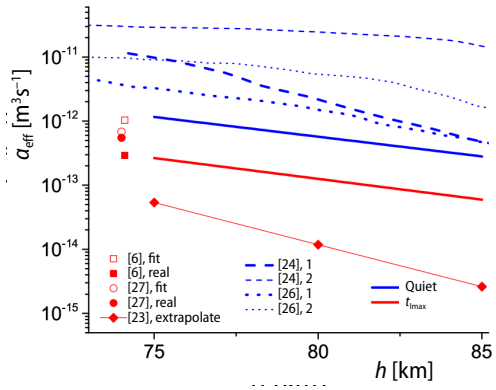

Figure 4. Altitude distribution of α_{eff} in a quiet state and at time of the X-ray flux maximum obtained in our model and their comparison with curves presented in [24, 25] for quiet conditions (blue lines) and presented or derived from data given in [6, 23, 26] for the maximum radiation (red line or scatters). Detailed description is given in text (*for color image see journal web site*)

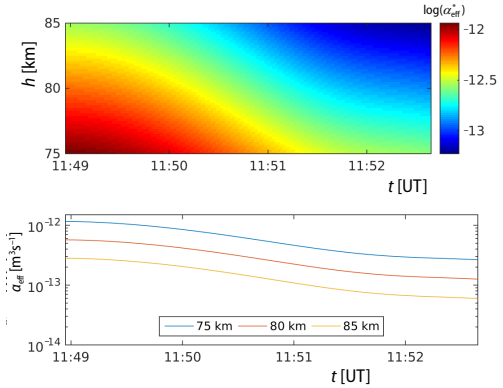

Figure 5. Upper panel: Surface plot α_{eff} normalized to its unit values 1 m^{3}s^{-1} as a function of time, *t*, and altitude, *h*, during increase of the X-ray flux of the considered solar X-ray flare. Bottom panel: Time evolution of α_{eff} at altitudes of 75 km, 80 km and 85 km during increase of the X-ray flux of the considered solar X-ray flare (*for color image see journal web site*)

(blue dotted lines). Comparison with one curve given in [24] (tick dashed blue line) is better for higher altitudes while the second curve given in [24] (thin dashed blue line) has larger values of α_{eff} than in the cases of all presented dependencies (this deviation is more pronounced at higher altitudes).

Comparison of the obtained dependence $\alpha_{eff}(h)$ at the moment of the X-radiation maximum is harder than for quiet condition because of the lack of relevant data for the X-ray flares of the considered class. In fig. 4 we show the relevant data for 74.1 km and 74 km obtained by fitting of dependencies α_{eff} in the maximum X-radiation flux presented in [6, 27] (fill and open scatters, respectively). In addition, in these studies we give calculated values for events of class very similar to the X-ray flare which we analyze. Here, one can see that all these values and the expected value in our calculation which can be seen as extrapolation of the red line to 74 km, differ within one order of magnitude. The lower values of $\alpha_{eff}(h)$ are obtained by extrapolation of data presented in [23] (red line with scatters). In this case better comparison is obtained for lower altitude (within one order of magnitude below about 80 km). At 85 km, these values are within two orders of magnitude.

Time evolutions of the effective recombination coefficient, α_{eff}, in altitude domain between 75 km and 85 km during the period of the X-ray flux increase are presented in fig. 5 for the considered flare. The upper panel shows that both time and altitude dependences are monotonous functions. Namely, the values of α_{eff} at fixed altitude decrease during the entire considered period and, on the other side, they increase going to the Earth surface at a fixed time, *t*.

Time evolutions of α_{eff} at altitudes 75 km, 80 km and 85 km are shown in the bottom panel of fig. 5. As one can see, the shapes of these dependences are the same for the logarithmic y scale and, for the considered X-ray flare event, their values differ within an order of magnitude at a fixed altitude.

Properties of the monotonous time and altitude dependences of the electron loss rate, calculated using eq. (10) for the known α_{eff} and N_e are opposite of what was obtained in the previous analysis. Namely, it can be seen in the upper panel of fig. 6 that this parameter reaches a

maximum at the end of the considered time interval and that its value increases with altitude during the entire time period.

Contrary to the same shapes of the time evolution of the parameter α_{eff} at different heights, the comparison of the electron loss rate during the considered time period at 75 km, 80 km, and 85 km shows a larger increase of its values going to the upper D-region boundary. According eq. (10), this difference can be explained by a more pronounced increase of the electron density ($L \sim N_e^2$) relative to the decrease of the effective recombination coefficient ($L \sim \alpha_{\text{eff}}$) occurring with altitude.

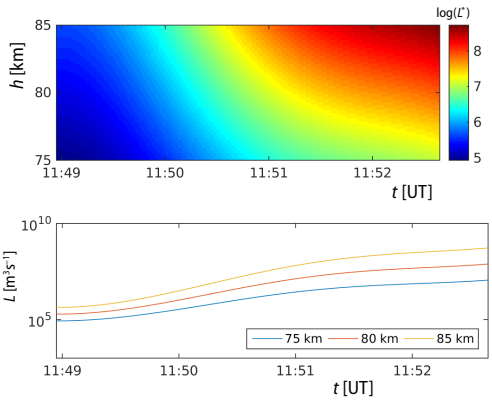

Figure 6. The same as in fig. 5 but for the electron loss rate *L* (*for color image see journal web site*)

Keeping in mind that the electron loss rate is approximatively equal to the electron gain rate induced by the Lyα radiation in the quiet period, we can say that the obtained values before the X-ray flare perturbation in this case are in agreement with values presented for the other two flares in [7] and those given in [24, 28, 29, 30]. Comparison of the noticed dependences are shown in [7]. In addition, as we already said, the electron density at the maximum of the X-radiation is in the domain of values reported in other papers (see for example [6, 9, 16]). For this reason and owing to the indicated agreement of the effective recombination coefficient, we can conclude that eq. (10) for the electron loss rate at the maximum of the X-radiation flux yields acceptable values.

Conclusions

In this study we presented a procedure for determination of changes of plasma parameters in the upper D-region during the increase of ionospheric heating by solar radiation during an X-ray flare. We considered the effective recombination coefficient and electron loss rate and apply the developed procedure to determine their time evolutions at the altitude domain between 75 km and 85 km from data obtained from the low ionospheric monitoring by the VLF signal emitted in Germany and received in Serbia during the influence of the solar X-ray flare which occurred on May 5, 2010.

The obtained results show a decrease of the effective recombination coefficient with strengthening of the X-radiation at altitudes between 75 and 85 km with the same profiles in the lin-exp scale. Nevertheless, the electron loss rate increases in time and with altitude. Also, the variations of this rate in the considered height domain increase in time, e.g. with the radiation flux.

This procedure includes data obtained in real observations which indicates the relevance of obtained results for research of the considered part of the D-region and the considered event that cause perturbations. It is an extension of research of plasma parameters to D-region during influence of a solar X-ray flare. Namely, the existing studies are primarily directed to the quiet conditions before the flare occurrence, at radiation flux maximum, or in the relaxation period after termination of the flare influence on the atmosphere. Our results, however, introduce the effects of temporal transition between the first two quasi stationary states and can also be used for modeling the temporal transition to the third domain (between the radiation flux maximum and beginning of the relaxation period) which, to our knowledge, has not yet been done from real observation data.

Because this method is applicable to numerous data sets obtained by the VLF/LF receiver network (it observes a large part of the terrestrial low ionosphere), the presented procedure allows further studies of spatial variation of the considered ionospheric parameters and enables research of influence of different spectral properties of solar X-ray flare events. The obtained results also open a possibility for modeling parameters relevant to electron gain processes using the equation for electron density dynamics. Here, we point out that this research requires a detailed analysis of the influence of the X-ray photon energies on the upper D-region altitude domain and that inclusion of time evolution of the X-radiation should be analyzed in more details for a better determination of these parameters.

Acknowledgment

The authors thank the Ministry of Education, Science and Technological Development of the Republic of Serbia through the projects III 44002 176001, 176002, 176004 and III47007. The data for this paper collected by the GOES-14 satellite is available at NOAA's National Centers for Environmental information (http://satdat.ngdc.noaa.gov/sem/goes/data/new_full/2010/05/goes14/csv). Requests for the VLF data used for analysis can be directed to the corresponding author.

Nomenclature

A_{rec} – recorded signal amplitude
C – normalized coefficient
G_0 – electron gain rate under unperturbed conditions, [m^3s^{-1}]
H' – signal reflection height, [km]
h – altitude [km]
I – X-radiation flux, [Wm^{-2}]
K – scaling coefficient, [$W^{-1}m^{-1}s^{-1}$]
L – electron loss rate, [m^3s^{-1}]
N_e – electron density, [Wm^{-2}]
P_{rec} – recorded signal phase
r – correction coefficient, [–]
t – time, [s]

Greek letters

α_{eff} – effective recombination coefficient, [m^3s^{-1}]
β – sharpness, [km^{-1}]
ψ_{eff} – fitted effective recombination coefficient, [m^3s^{-1}]

Superscripts

* – normalized on unique values
o – unperturbed conditions

Acronyms

AWESOME – atmospheric weather electromagnetic system for observation modelling and education
LWPC – long-wave propagation capability
VLF – very low frequency

References

[1] Singh, A. K., *et al.*, Solar Flare Induced D-region Ionospheric Perturbations Evaluated from VLF Measurements, *Astrophysics and Space Science, 350* (2014), 1, pp. 1-9
[2] Srećković, V. A., *et al.*, The Effects of Solar Activity: Electrons in the Terrestrial Lower Ionosphere, *Journal of the Geographical Institute "Jovan Cvijic" SASA, 67* (2017), 3, pp. 221-233
[3] Todorović Drakul, M., *et al.*, Behaviour of Electron Content in the Ionospheric D-region During Solar X-ray Flares, *Serbian Astronomical Journal, 2016* (2016), 193, pp. 11-18
[4] Nina, A., *et al.*, Diagnostics of Plasma in the Ionospheric D-region: Detection and Study of Different Ionospheric Disturbance Types, *European Physical Journal D, 71* (2017), 7, 189
[5] Nina, A., *et al.*, Analysis of the Relationship Between the Solar X-ray Radiation Intensity and the D-region Electron Density Using Satellite and Ground-based Radio Data, *Solar Physics, 293* (2018), Apr., 64
[6] Žigman, V., *et al.*, D-region Electron Density Evaluated from VLF Amplitude Time Delay During X-ray Solar Flares, *Journal of Atmospheric and Solar-Terrestrial Physics, 69* (2007), 7, pp. 775-792
[7] Nina, A., Čadež, V. M., Electron Production by Solar Ly-α Line Radiation in the Ionospheric D-region, *Advances in Space Research, 54* (2014), 7, pp. 1276-1284

[8] Bajčetić, J., *et al.*, Ionospheric D-region Temperature Relaxation and its Influences on Radio Signal Propagation after Solar X-flares Occurrence, *Thermal Science, 19* (2015), Suppl. 2, pp. S299-S309
[9] Thomson, N. R. *et al.*, Large Solar Flares and their Ionospheric D Region Enhancements, *Journal of Geophysical Research (Space Physics), 110* (2015), A6, pp. A06306: 1-10
[10] Ferguson, J. A., *Computer Programs for Assessment of Long-Wavelength Radio Communications*, Version 2.0, Space and Naval Warfare Systems Center, San Diego, Cal., USA, 1998
[11] Woods, T. N., *et al.*, New Solar Extreme-ultraviolet Irradiance Observations, *The Astrophysical Journal, 739* (2011), 2, pp. 59-71
[12] Cohen, M. B., *et al.*, Sensitive Broadband ELF/VLF Radio Reception with the AWESOME Instrument, *IEEE Transactions on Geoscience and Remote Sensing, 48* (2010), 1, pp. 3-17
[13] Radovanović, M, Investigation of Solar Influence on the Terrestrial Processes: Activities in Serbia, *Journal of the Geographical Institute "Jovan Cvijic" SASA, 68* (2018), 1, pp. 149-155
[14] Wait, J. R., Spies, K. P., Characteristics of the Earth-Ionosphere Waveguide for VLF Radio Waves, NBS Technical Note, Col., USA, 1964
[15] Thomson, N. R, Experimental Daytime VLF Ionospheric Parameters, *Journal of Atmospheric and Terrestrial Physics, 55* (1993), 2, pp. 173-184
[16] Grubor, D. P., *et al.*, Classification of X-ray Solar Flares Regarding their Effects on the Lower Ionosphere Electron Density Profile, *Annales Geophysicae, 26* (2008), 7, pp. 1731-1740
[17] Kumar, S., *et al.*, Perturbations to the Lower Ionosphere by Tropical Cyclone Evan in the South Pacific Region, *Journal of Geophysical Research: Space Physics, 122* (2017), 8, pp. 8720-8732
[18] Nina, A., *et al.*, Altitude Distribution of Electron Concentration in Ionospheric D-region in Presence of Time-varying Solar Radiation Flux, *Nuclear Instruments and Methods in Physics Research B, 279* (2012), May, pp. 110-113
[19] Kolarski, A., Davorka Grubor, D., Sensing the Earth's Low Ionosphere During Solar Flares Using VLF Signals and GOES Solar X-ray Data, *Advances in Space Research, 53* (2014), 11, pp. 1595-1602
[20] McEwan, M., Phillips, F., *Chemistry of the Atmosphere*, Mir, Moscow, Russia, 1978
[21] Blaunstein, N., Christodoulou, C., *Radio Propagation and Adaptive Antennas for Wireless Communication Links: Terrestrial, Atmospheric and Ionospheric*, John Wiley and Sons, Inc., Hoboken, New Jersey, 2006
[22] Deshpande, S. D., Mitra, A. P., Ionospheric Effects of Solar Flares – III. the Quantitative Relationship of Flare X-rays to SID's, *Journal of Atmospheric and Terrestrial Physics, 34* (1972), 2, pp. 243-253
[23] Hayes, L. A., *et al.*, Pulsations in the Earth's Lower Ionosphere Synchronized with Solar Flare Emission, *Journal of Geophysical Research: Space Physics, 122* (2017), 10, pp. 9841-9847
[24] Mitra, A. P., *Ionospheric Effects of Solar Flares*, Mir, Moscow, Russia, 1974
[25] Sato, T., The Response of the Lower Ionosphere to the Great Solar Flare of August 7, 1972, *Journal of Geomagnetism and Geoelectricity, 27* (1975), 5, pp. 383-407
[26] Osepian, A., *et al.*, D-region Electron Density and Effective Recombination Coefficients During Twilight – Experimental Data and Modelling During Solar Proton Events, *Annales Geophysicae, 27* (2009), 10, pp. 3713-3724
[27] Basak, T., Chakrabarti, S. K., Effective Recombination Coefficient and Solar Zenith Angle Effects on Low-latitude D-Region Ionosphere Evaluated from VLF Signal Amplitude and its Time Delay During X-ray Solar Flares, *Astrophysics and Space Science, 348* (2013), 2, pp. 315-326
[28] Rowe, J. N., Model Studies of the Lower Ionosphere, Sci. Rep.No. 406, Pennsylvania State Univ., Univ. Park, Penn., USA, 1972
[29] Aikin, A. C., *et al.*, Some Results of Rocket Experiments in the Quiet D Region, *Journal of Geophysical Research, 69* (1964), 21, pp. 4621-4628
[30] Bourdeau, R. E., *et al.*, The Lower Ionosphere at Solar Minimum, Greenbelt, Md.: NASA, Goddard Space Flight Center. 1965

Paper submitted: May 1, 2019
Paper revised: July 10, 2019
Paper accepted: July 11, 2019